

Clouded Crystal Ball Analysis of the Inelastic Scattering Cross Section of a Neutron into the Isomeric Level (13/2⁺) of ⁸²Pb²⁰⁷†

SOPHIE OLEKSA

Brookhaven National Laboratory, Upton, New York

(Received October 28, 1955)

The clouded crystal ball model was used in the calculation of the cross section for excitation of the 0.8-sec metastable state of ⁸²Pb²⁰⁷ (Stelson and Campbell's experimental data). Values of X_0^2 were varied from 140 to 172, two values of ζ were considered, $\zeta=0.03$ and $\zeta=0.05$, and two values of the radius, $R=1.45A^{1/3} \times 10^{-13}$ cm and $R=(1.27A^{1/3}+0.7) \times 10^{-13}$ cm. The clouded crystal ball model and the strong-interaction model both fit the experimental data. The former, however, is extremely sensitive to changes in the parameter X_0^2 . The radius $R=1.45A^{1/3} \times 10^{-13}$ cm fits the data better than $R=(1.27A^{1/3}+0.7) \times 10^{-13}$ cm.

I. INTRODUCTION

IN their development of the theory for the inelastic scattering of neutrons, Hauser and Feshbach¹ used a compound nucleus model with a statistical distribution of levels for the compound states. Margolis² used this theory with considerable success in applying the strong-interaction model³ to the excitation of metastable nuclear states by the inelastic scattering of monoenergetic neutrons. Feshbach, Porter, and Weisskopf⁴ later proposed a clouded crystal ball model which was particularly applicable in the calculations of total cross sections and angular distributions. Thus far, little has been done about the application of the clouded crystal ball model to inelastic scattering data.^{5,6} We have, therefore, used this model to calculate the cross sections found experimentally by Stelson and Campbell for the excitation of the 0.8-sec metastable state of ⁸²Pb²⁰⁷ by inelastic scattering of neutrons.⁷ Stelson and Campbell have already fitted these data successfully by means of the strong-interaction model. We are interested in seeing how sensitive the clouded crystal ball model is for inelastic scattering and whether parameters different from those used to fit total cross-section data are needed to fit the inelastic scattering data. We are also interested in how much the clouded crystal ball model differs in its predictions from the strong-interaction model.

II. THEORY

Hauser and Feshbach derived the following expression for the inelastic scattering cross section for a neutron of initial energy E from the target nucleus with spin i to a neutron with final energy E' and a residual nucleus

with spin i' :

$$\sigma_{in}(i|i') = \frac{\pi \lambda^2}{2(2i+1)} \sum_l T_l(E) \times \sum_{j,l'} \frac{\epsilon_{j,l'}^J (2J+1)}{1 + \frac{\sum_{j'',l'',q} \epsilon_{j'',l'',q}^J T_{l''}(E_q') / \sum_{l',j'} \epsilon_{j',l'}^J T_{l'}(E')}{}}$$
 (1)

where J = the spin of a level in the compound nucleus, $\lambda = \lambda/2\pi = 1/k$, k , the wave number, $= 0.22(M/M+1)E^{1/2} \times 10^{13}$ cm⁻¹ with E in Mev, M = mass of target nucleus and in neutron masses, $j_{1,2} = i \pm \frac{1}{2}$

$$\epsilon_{j,l'}^J = \begin{cases} 2, & \text{if both } j_1 \text{ and } j_2 \text{ satisfy} \\ 1, & \text{if either } j_1 \text{ or } j_2 \text{ but not both satisfy} \\ 0, & \text{if neither } j_1 \text{ nor } j_2 \text{ satisfies} \end{cases} \quad |J-l| \leq j_i \leq (J+l)$$
 (2)

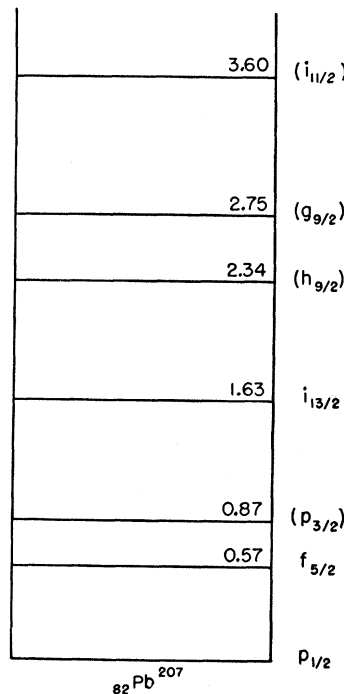


FIG. 1. Energy level diagram of the low-lying levels of ⁸²Pb²⁰⁷. The spins given in parentheses were not determined experimentally but come from shell structure considerations.

† Research performed under the auspices of the U. S. Atomic Energy Commission.

¹ W. Hauser and H. Feshbach, Phys. Rev. **87**, 366 (1952).

² B. Margolis, Phys. Rev. **93**, 204 (1953).

³ Feshbach, Peaslee, and Weisskopf, Phys. Rev. **71**, 145 (1947); H. Feshbach and V. F. Weisskopf, Phys. Rev. **76**, 1550 (1949).

⁴ Feshbach, Porter, and Weisskopf, Phys. Rev. **90**, 166 (1953); **96**, 448 (1954).

⁵ S. Oleksa, Brookhaven National Laboratory Report BNL-273 (T-45), 1953 (unpublished).

⁶ J. J. VanLoef and D. A. Lind, Phys. Rev. **101**, 103 (1956).

⁷ P. H. Stelson and E. C. Campbell, Phys. Rev. **97**, 1222 (1955).

Equation (1) includes the competition due to capture elastic scattering and the inelastic scattering of the neutrons by other levels. It does not take into consideration the (n,γ) process or emission of particles other than neutrons since, in the energy range we consider, these events are very small compared to neutron emission. The j'' refers to all possible final channel spins, the l'' to all possible final neutron orbital angular momenta, and the E_q' to all possible final neutron energies. The j' refers to the two values of the final channel spin, the l' to all values of the orbital angular momenta of the neutrons emerging from the particular excited state that is being considered, and E' to the final energy of these neutrons. The prime in

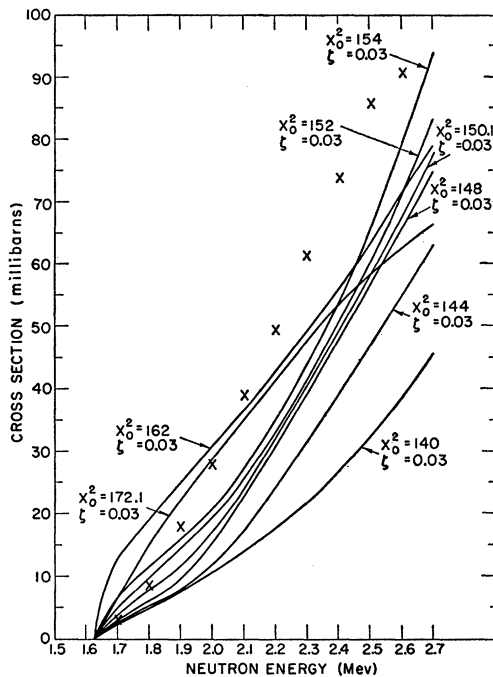


FIG. 2. Calculated cross sections based on the clouded crystal ball model for $\zeta=0.03$ and $R=1.454 \times 10^{-13}$ cm. The parameter X_0^2 is varied from 140 to 172.1; the \times 's are Stelson and Campbell's experimental points.

the sum requires the omission of those terms for which $E_q' = E'$, $l'' = l'$, and $j'' = \text{either value of } j'$. In other words, the sums are over all the energy levels of the residual nucleus, over all the residual channel spins and all the angular momenta which are possible, excluding, however, the level to which the decay proceeds. The values pertaining to the level to which the decay proceeds are found in $\sum_{\nu, j'} \epsilon_{j'} \nu^j T_{\nu}(E')$. Conservation of parity leads to the fact that all even l' or all odd l' are found in this expression.

The $T_l(E)$ are transmission coefficients which show what fraction of the bombarding particles penetrate into $r < R$, where R equals the nuclear radius. Blatt and

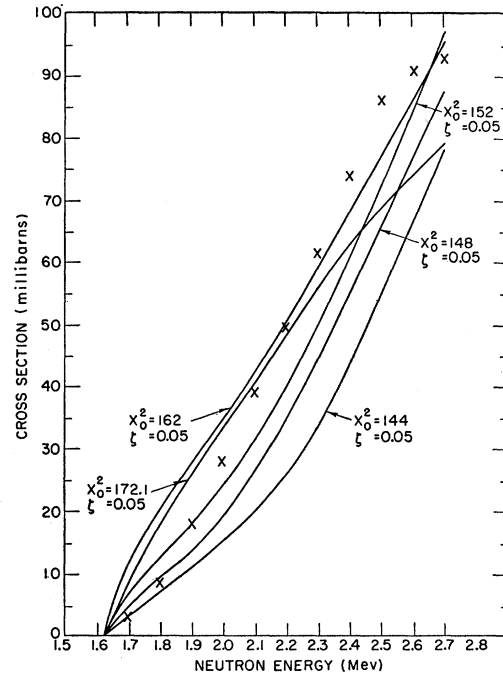


FIG. 3. Calculated cross sections based on the clouded crystal ball model for $\zeta=0.05$ and $R=1.454 \times 10^{-13}$ cm. The parameter X_0^2 is varied from 144 to 172.1. The \times 's are the experimental points.

Weisskopf⁸ show that

$$T_l(E) = \frac{-4s_l \text{Im}f_l}{(\text{Re}f_l - \Delta_l)^2 + (\text{Im}f_l - s_l)^2}, \quad (3)$$

with $\Delta_l + is_l = 1 + xh_l'(x)/h_l(x)$, where $x = R/\lambda = kR$ and $h_l(x)$ is a spherical Hankel function of the first kind. f_l is the logarithmic derivative of the wave function at the boundary; $\text{Re}f_l$ is the real part of f_l and $\text{Im}f_l$ is its imaginary part. The form of f_l depends upon the model used. In the strong-interaction model, the nucleon upon entering the target nucleus immediately forms a compound nucleus in which its motion is completely integrated with the motions of all the other nucleons into a collective whole. Here f_l is approximately equal to $-iKR$,⁹ where $(KR)^2 = (kR)^2 + (K_0R)^2 = x^2 + X_0^2$. K_0 is the wave number of the particle within the nucleus for zero incident energy. The clouded crystal ball model suggests more of a shell structure which permits the nucleon to exist as an individual particle for some time before it is absorbed into a compound nucleus. It is described by a complex square-well potential of the form

$$\begin{aligned} V(r) &= -V_0(1+i\zeta) & \text{for } r < R, \\ V(r) &= 0 & \text{for } r > R, \end{aligned} \quad (4)$$

⁸ J. M. Blatt and V. F. Weisskopf, *Theoretical Nuclear Physics* (John Wiley and Sons, Inc., New York, 1952), p. 334.

⁹ The logarithmic derivative f_l here is not quite equal to $-iKR$. It should be the limit obtained from the clouded crystal ball model for a large ζ . The numerical results, however, are not affected if one uses $f_l = -iKR$.

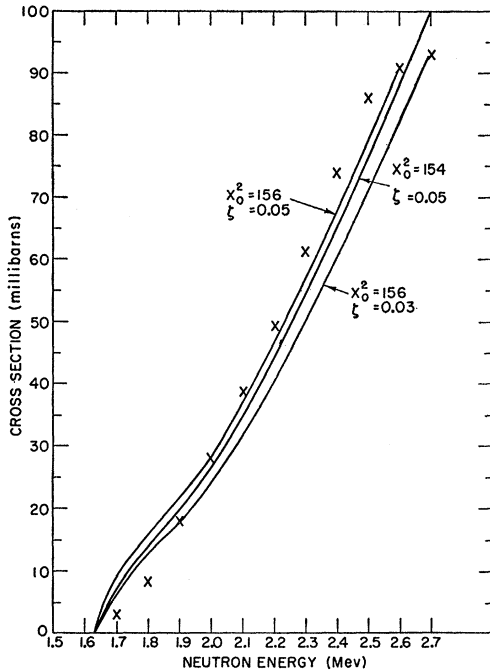


FIG. 4. Calculated cross sections based on the clouded crystal ball model which best fit the experimental data indicated by the \times 's. $R=1.45A^{1/3}\times 10^{-13}$ cm.

where V_0 = the depth of the well, ζ determines the amount of independence and is related to the absorption probability. For $\zeta=0$, the clouded crystal ball model reduces to the independent-particle model; for $\zeta \approx 0.1$, the clouded crystal ball model approaches the strong-interaction model. f_l here is equal to $1 + X j_l'(X)/X$, where $j_l(X)$ is the spherical Bessel function and $X^2 = x^2 + X_0^2(1 + i\zeta)$ with $X_0^2 = (2m/\hbar^2)V_0R^2 = K_0^2R^2$ and $x^2 = (2m/\hbar^2)ER^2 = k^2R^2$; m is the reduced neutron mass and E is the energy of the incoming neutron. The calculations in this paper have been done in terms of the parameters X_0^2 , x , and ζ .

III. CALCULATIONS

The assignments of spins, parities, and energies to the low-lying states of ${}_{82}\text{Pb}^{207}$ are shown in Fig. 1.⁷ The spins given in parentheses were not determined experimentally but come from shell structure considerations. In Fig. 2, the experimental data of Stelson and Campbell are given; the absolute values are correct to ± 40 percent. Although their experimental data go up to 3.1 Mev, in Fig. 2 they are shown only up to 2.7 Mev. This is so because our calculations are valid only up to 2.5–2.6 Mev. Because of the uncertainties in spin assignments we did not include any state higher than the $13/2^+$ state. There is a level at 2.34 Mev but its effects up to 2.5 Mev are small. For these calculations values of the angular momenta up to $l=6$ were included.

In Figs. 2, 3, and 4 we show how the calculations

with the clouded crystal ball model fit the experimental data. The calculations in Fig. 2 were done for $R=1.45A^{1/3}\times 10^{-13}$ cm, $\zeta=0.03$ and X_0^2 varying from 140 to 172; the calculations in Fig. 3 were done for $R=1.45A^{1/3}\times 10^{-13}$ cm, $\zeta=0.05$ and X_0^2 varying from 144 to 172. $X_0^2=144$ corresponds to a well depth of 41 Mev instead of the value 20 Mev used in earlier clouded crystal ball calculations³ because Feshbach, Porter, and Weisskopf⁴ and Adair¹⁰ found that the former value gives a better fit to the total cross-section data. It can be seen from these figures that the clouded crystal ball model is extremely sensitive to the choice of X_0^2 , which is proportional to the product of the well depth and radius squared. A small change in X_0^2 (really in the depth of the potential well since the same radius is used) can affect the cross section significantly. A comparison of Figs. 2 and 3 show what effect a change in ζ from 0.03 to 0.05 has. In Fig. 4, we show the best fit to the experimental data. These curves were obtained by interpolation from the curves in Figs. 2 and 3.

In Fig. 5, we show the results of the strong-interaction model. Stelson and Campbell were able to fit their experimental data with $X_0^2=64$ ($R=8.0\times 10^{-13}$ cm and $K=1\times 10^{13}$ cm⁻¹ which is equivalent to a well depth of 20 Mev). In the same figure, we fit the data with the same model but with $X_0^2=144$ and $R=1.45A^{1/3}\times 10^{-13}$ cm ($R=8.58\times 10^{-13}$ cm). Again the fit is a good one. The agreement between the two calculations is fortuitous. Isolated points, however, were checked for $X_0^2=140, 148, \text{ and } 152$ for $R=1.45A^{1/3}\times 10^{-13}$ cm. The

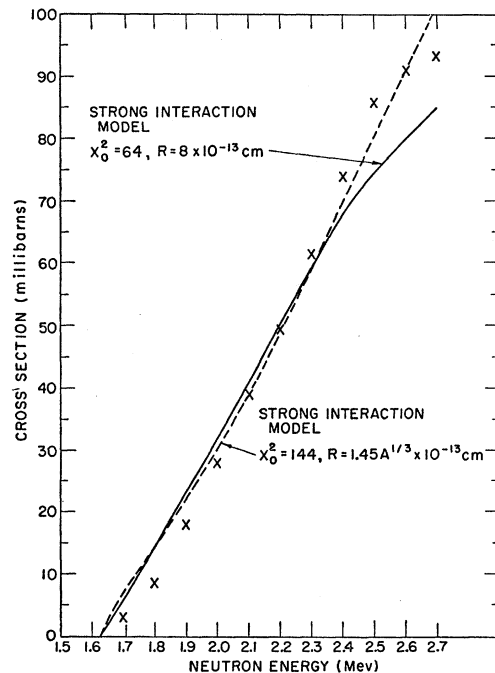


FIG. 5. Calculated cross sections based on the strong-interaction model. The \times 's are the experimental point.

¹⁰ R. K. Adair, Phys. Rev. 94, 737 (1954).

differences between these values and those obtained for $X_0^2=144$ were negligible. Unlike the clouded crystal ball model, the strong-interaction model is not too sensitive to changes in X_0^2 .

Recent analyses¹¹ of the cross-section data indicate that a better radius for the square-well model is $R=(1.27A^{1/3}+0.7)\times 10^{-13}$ cm ($R=8.22\times 10^{-13}$ cm). In Fig. 6, we compare the results obtained for $R=1.45A^{1/3}\times 10^{-13}$ cm and $R=(1.27A^{1/3}+0.7)\times 10^{-13}$ cm for $X_0^2=152$, $\zeta=0.05$, $X_0^2=154$, $\zeta=0.03$, and $X_0^2=144$ for the strong-interaction model. In each case, the larger radius gives a better fit to the experimental data.

IV. CONCLUSIONS

Both models fit the experimental data for a radius of $R=1.45A^{1/3}\times 10^{-13}$ cm. They differ, however, in their sensitivity to changes in X_0^2 . The clouded crystal ball model is particularly sensitive to this parameter, the strong-interaction model much less so. This is to be ascribed to the differences in the penetrability coefficients. The $T_i(E)$ values for the strong-interaction model are all the same form and smoothly approach an asymptotic value. A 5 percent change in X_0^2 would not affect the shape of the curves and would not make much difference in the absolute values. The $T_i(E)$ values for the clouded crystal ball model, however, do not rise smoothly to an asymptotic value but have

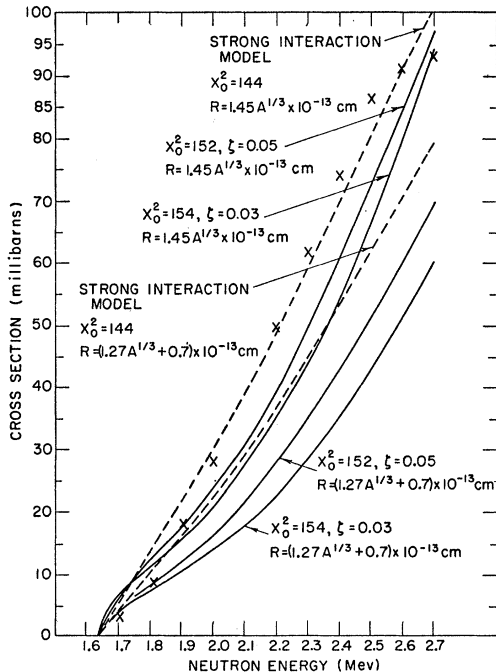


FIG. 6. Comparison of the calculated cross sections for $R=1.45A^{1/3}\times 10^{-13}$ cm and $R=(1.27A^{1/3}+0.7)\times 10^{-13}$ cm. The \times 's are the experimental points.

¹¹ V. F. Weisskopf, Proceedings of the International Conference on the Peaceful Uses of Atomic Energy, Geneva, 1955 (unpublished).

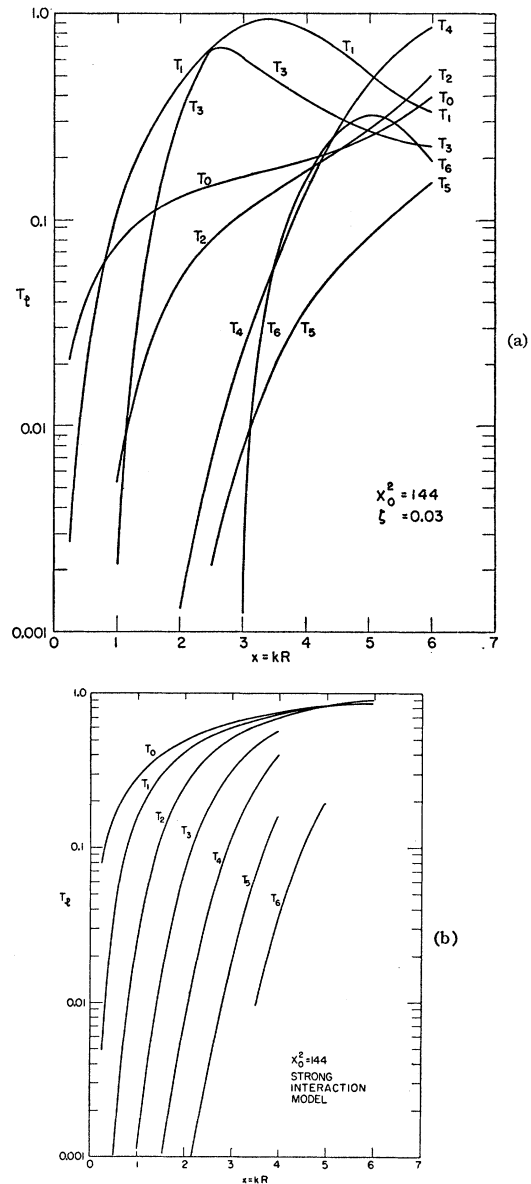


FIG. 7. Comparison of $T_i(E)$ values for the clouded crystal ball model and the strong-interaction model.

peaks and valleys. The positions and shapes of these peaks and valleys depend sensitively on the potential well and radius. A 5 percent change in X_0^2 could easily shift or depress a peak. A comparison of the $T_i(E)$ values for both models is shown in Fig. 7.

The clouded crystal ball model was most successful in the calculations of total cross sections and angular distributions. Total cross-section data led to the selection of $\zeta=0.03$ in preference to the original value of $\zeta=0.05$. Within the errors of calculation (estimated to be about 10 percent) the inelastic scattering cross section for this particular level does not distinguish between $\zeta=0.05$ and $\zeta=0.03$. The calculations with

the parameter $\zeta=0.05$ fit the data as well as the results for $\zeta=0.03$. Because of the large experimental error quoted by Stelson and Campbell, for a particular ζ we varied the X_0^2 so that the results would bracket the experimental data. $\zeta=0.05$ fits the data for a slightly smaller well depth V_0 better than does $\zeta=0.03$.

With the square-well model, the most recent total cross-section data indicate that for lead the smaller radius of $R=(1.27A^{1/3}+0.7)\times 10^{-13}$ cm is to be preferred to $R=1.45A^{1/3}\times 10^{-13}$ cm. For the calculation of the inelastic scattering cross section into the isomeric level of ${}_{82}\text{Pb}^{207}$, the opposite is true, i.e., the larger radius seems to be preferred as can be seen in Fig. 6. In

Fig. 6, we kept X_0^2 constant. Had we kept V_0 constant, the difference between the results would have been greater, with the larger radius even more favored. The strong-interaction model gives the same result so far as the size of the radius is concerned.

ACKNOWLEDGMENTS

I wish to thank Charles E. Porter for many helpful discussions, Robert G. Thomas of Los Alamos for sending me the penetrability factors, Bernard Mozer and William Bornstein for assistance with the calculations, and P. H. Stelson and E. C. Campbell for giving me their experimental data before publication.

Nuclear Levels and Transitions in Lu^{175} According to the Unified Model*

DAVID M. CHASE AND LAWRENCE WILETS

Los Alamos Scientific Laboratory, University of California, Los Alamos, New Mexico

(Received September 1, 1955)

The scheme for the decay of Yb^{175} and Hf^{175} to Lu^{175} is analyzed theoretically on the basis of the Bohr-Mottelson strong-coupling unified model. A set of spins and parities for all the levels involved is found to be uniquely consistent with the available experimental data and the level-structure predictions of the model. The anomalously large ratio of $M2$ to $E1$ radiation observed in two of the gamma transitions is accounted for as a consequence of configuration forbiddenness. Parallel remarks are made concerning the spectrum of Hf^{177} .

1. INTRODUCTION

RECENTLY, a rather detailed experimental investigation of the decay of Yb^{175} and Hf^{175} to the low-lying levels of Lu^{175} has been performed by Mize, Bunker, and Starner.¹ The Yb decay has been studied also by de Waard,² Akerlind, Hartmann, and Wiedling,² and Marty³ and the Hf decay by Burford, Perkins, and Haynes.⁴ Since these nuclei lie in a region of large deformation, the strong-coupling unified model⁵ may be expected to provide useful guidance in the interpretation of the level structure and characteristic features of the decay scheme. Conversely, the example furnishes an opportunity to subject the model to further experimental test.

Relevant essentials of the strong-coupling unified model are here briefly recalled. For axially symmetric nuclei the component K of the total nuclear angular momentum I along the symmetry axis is supposed to be an approximately good quantum number. For an odd- A nucleus the rotational band based on a particular

intrinsic structure is constituted of levels with spin sequence $I=K, K+1, K+2, \dots$, all of the same parity as the intrinsic structure. The rotational energies are given by

$$W_{\text{rot}} = (\hbar^2/2\mathcal{I})[I(I+1) - K(K+1)], \quad (1)$$

except in the special case $K=\Omega=1/2$, \mathcal{I} being the moment of inertia. In the low-lying levels encountered here, there is no vibrational excitation, whence $K=\Omega$, where Ω is the sum of the components of the angular momenta of unpaired nucleons along the nuclear symmetry axis; also, no more than a single nucleon is excited, whence Ω is equal to the contribution of the odd nucleon only. States of an odd nucleon are conveniently identified (in the independent-particle approximation) by Ω , l , and j , the last two being good quantum numbers only in the limit of zero deformation.

Calculations by Nilsson⁶ of independent-particle energy levels and wave functions for a spheroidal well with spin-orbit coupling have made possible a more detailed and unambiguous application of the strong-coupling model.⁷ His energy levels as functions of deformation are shown in Fig. 2.

* Work performed under the auspices of the U. S. Atomic Energy Commission.

¹ Mize, Bunker, and Starner, *Phys. Rev.* **100**, 1390 (1955); hereafter referred to as MBS.

² H. de Waard, *Phil. Mag.* **46**, 445 (1955); Akerlind, Hartmann, and Wiedling, *Phil. Mag.* **46**, 448 (1955).

³ N. Marty, *Compt. rend.* **240**, 963 (1955).

⁴ Burford, Perkins, and Haynes, *Phys. Rev.* **99**, 3 (1955).

⁵ A. Bohr and B. R. Mottelson, *Kgl. Danske Videnskab. Selskab, Mat.-fys. Medd.* **27**, No. 16 (1953).

⁶ S. G. Nilsson, *Kgl. Danske Videnskab. Selskab, Mat.-fys. Medd.* **29**, No. 16 (1955).

⁷ A survey of ground and low excited states of deformed nuclei based on these calculations has been made by B. R. Mottelson and S. G. Nilsson [*Phys. Rev.* **99**, 1615 (1955)].